Molecular Endocrinology. First published ahead of print August 26, 2013 as doi:10.1210/me.2013-1109

AMPK regulates ER morphology and function in stressed pancreatic β-cells *via* phosphorylation of DRP1

Jakob D. Wikstrom[1], Tal Israeli[1], Etty Bachar-Wikstrom[1], Avital Swisa[2], Yafa Ariav[1], Meytal, Waiss[3], Daniel Kaganovich[3], Yuval Dor[2], Erol Cerasi[1], Gil Leibowitz[1]

[1]Endocrinology and Metabolism Service, Department of Medicine, Hadassah-Hebrew University Medical Center, [2]Department of Developmental Biology and Cancer Research, The Institute for Medical Research Israel-Canada (IMRIC), [3]Department of Cell and Developmental Biology, Alexander Silberman Institute of Life Sciences, The Hebrew University; The Hebrew University-Hadassah Medical School, Jerusalem, Israel.

Experimental lipotoxicity constitutes a model for β-cell demise induced by metabolic stress in obesity and type 2 diabetes. Fatty-acid excess induces ER stress, which is accompanied by ER morphological changes whose mechanisms and relevance are unknown. We found that the GTPase DRP1, a key regulator of mitochondrial fission, is an ER resident regulating ER morphology in stressed β-cells. Inhibition of DRP1 activity using a GTP hydrolysis-defective mutant (Ad-K38A) attenuated fatty acid-induced ER expansion and mitochondrial fission. Strikingly, stimulating the key energy-sensor AMPK increased the phosphorylation at the anti-fission site Serine-637 and largely prevented the alterations in ER and mitochondrial morphology. Expression of a DRP1 mutant resistant to phosphorylation at this position partially prevented the recovery of ER and mitochondrial morphology by AMPK. Fatty acid-induced ER enlargement was associated with proinsulin retention in the ER, together with increased proinsulin/insulin ratio. Stimulation of AMPK prevented these alterations, as well as mitochondrial fragmentation and apoptosis. In summary, DRP1 regulation by AMPK delineates a novel pathway controlling ER and mitochondrial morphology, thereby modulating the response of β-cells to metabolic stress. DRP1 may thus function as a node integrating signals from stress regulators, such as AMPK, to coordinate organelle shape and function.

The endoplasmic reticulum (ER) is the site of proinsulin biosynthesis and folding, and thus plays an important role in insulin production and secretion (1). Considering the vital functions of the ER in β-cells, it may be expected that ER dysfunction plays an imperative role in the pathophysiology of type 2 diabetes (T2D); indeed, recent studies assign an important role to the ER in the development of β-cell failure (2).

Accumulation of misfolded proteins in the ER results in ER stress and consequently activation of the unfolded protein response (UPR). The latter is an adaptive signaling cascade aimed to decrease ER protein load and enhance folding capacity, while continuous UPR activation may lead to apoptosis (3). Morphological alterations of the ER alongside increased expression of UPR markers in β-cells have been documented in animal models of diabetes and humans with T2D (4, 5). ER stress is often accompanied by changes in ER morphology; however, the mechanisms involved and the impact of ER morphology on cellular function are poorly understood (6, 7).

The ER consists of a membrane network surrounding the nucleus and forming tubular and flat or sack-like structures (called sheets or cisternae) in the cytoplasm (8). Several proteins involved in ER membrane curvature stabilization and in regulation of interconnections of ER tubules have been identified (9). Little is known about the

ISSN Print 0888-8809 ISSN Online 1944-9917
Printed in U.S.A.

Received April 16, 2013. Accepted August 19, 2013.

Abbreviations:

formation of cisternae, although some of the tubule-shaping proteins may also be involved in stabilizing the edges of these structures (10). The ER and mitochondria exhibit tightly coupled dynamics and have extensive contacts. A recent report suggested that ER tubules define the position of mitochondrial fission sites, preceding the recruitment of dynamin-related protein 1 (DRP1) (11). DRP1 is a ubiquitous protein involved in the regulation of mitochondrial fission in physiology and stress (12). The mechanisms that modify ER morphology in stressed mammalian cells are less identified. The saturated free fatty acid (FFA) palmitate has been shown to induce ER expansion and stress in several cell types including pancreatic β-cells (6, 7, 13). Palmitate-induced β-cell stress leads to dysfunction and apoptosis in vitro and in vivo (14); this may have implications for obesity and T2D that are often associated with elevated FFA concentrations (15).

Herein we studied the mechanisms involved in the regulation of ER morphology and function in β-cells, as well as the interactions with mitochondria under stressful conditions. We found that the cellular energy sensor AMPK regulates FFA-induced ER morphology changes, as well as mitochondrial fragmentation. We identified DRP1 as an ER resident protein, and show it is a downstream target of AMPK. Stimulation of AMPK inhibited DRP1, prevented ER and mitochondrial morphology changes, and improved β-cell function and survival under lipotoxic conditions.

Research design and Methods

Islet isolation and cell culture

Islets were isolated from 12-wk old male C57BL6 mice by collagenase injection to the bile duct. Animal use was approved by the Institutional Animal Care and Use Committee of the Hebrew University and the Hadassah Medical Organization. Human islets (from 4 donors aged 45 ± 9 y) were obtained from the Clinical Islet Laboratory (University of Alberta/Alberta Health Services, Edmonton, Canada). The islets were cultured 27–98 h prior to shipment to Israel in CMRL1066 media. β-Cell viability in the different isolations was 78%–85%. Islets were cultured intact overnight and then dispersed by 0.05 mg/ml trypsin (Biological Industries, Beit-Haemek, Israel) and plated on 8-chamber borosilicate plates (Nunc, Rochester, NY). RPMI-1640 culture media was supplemented with 10 mmol/l glucose, 10% FBS, 100 IU/ml penicillin, 100 μg/ml streptomycin and 2 mmol/l L-glutamine (Biological Industries) and used for islets. Experiments were performed after culture for 2–3 d at 37°C in a humidified atmosphere containing 5% CO_2.

INS-1E β-cells (passage 65–95) were grown in RPMI 1640 medium supplemented with 10% FBS, 1 mmol/l sodium pyruvate, 2 mmol/l L-glutamine, 10 mmol/l HEPES, 0.05 mmol/l 2-betamercaptoethanol, 100 IU/ml penicillin and 100 μg/ml streptomycin (Biological Industries). Mouse embryonic fibroblasts (MEFs) were grown in DMEM supplemented with 10% FBS, 100 IU/ml penicillin and 100 μg/ml streptomycin.

Reagents

The palmitate-BSA, methylpalmitate-BSA or oleate-BSA solutions were prepared by dissolving the sodium salt of FFA (Sigma, Rehovot, Israel) at a concentration of 10 mmol/l in 11% bovine serum albumin (BSA) (Sigma) in a stirred water bath at 37°C for 16 h. The FFA-BSA solution pH was adjusted to 7.4, filtered through a sterile 0.22 μm filter and stored at –20°C; it was diluted 1:20 in culture media before use. The molar ratio of FFA:BSA was 6:1. The following compounds were obtained from Sigma: BSA, thapsigargin, tunicamycin, palmitic acid, methylpalmitate, oleic acid, 5-amino-1-β-D-ribofuranosyl-imidazole-4-carboxamide (AICAR), metformin, and carbonyl cyanide 4-(trifluoromethoxy)phenylhydrazone (FCCP). AICAR and metformin were applied to cells overnight prior to exposure to FFA.

Fluorescent constructs and dyes

The following constructs were used to express fluorescent proteins: *GFP*-wild type and S656A *Drp1* construct (S637 in human DRP1), in which the serine residue was substituted by alanine (Stefan Strack, University of Iowa, IA) (16), *eYfp-ER* (Clontech, Mountain View, CA), *Rfp-ER* (Felipe Pimentel Muinos, University of Salamanca, Spain) (17), *Gfp-proinsulin* (Louis Philipson, University of Chicago, IL) (18), *mCherry-calnexin* (Volodymyr Korkhov, ETH Zurich, Switzerland) (19), turquoise-ER (Dorus Gadella, Swammerdam Institute for Life Sciences, Netherlands) (20). Mitochondria were labeled with the fluorescent dyes tetramethylrhodamine-ethyl-ester (TMRE) (10 nmol/l, 1 h preincubation, present during imaging) or Mitotracker Red (200 nmol/l, 30 min incubation, washed-out prior to imaging) (Invitrogen, Carlsbad, CA).

Viruses

Adenovirus for expression of human AMPKα1 dominant negative and CMV null as control was purchased from Applied Biological Materials (Richmond, BC, Canada) and used 3 d after infection at MOI 100. Inhibition of AMPK activity was verified by Western blotting for phosphorylated acetyl-CoA carboxylase (ACC). Adenovirus for expression of DRP1 dominant negative (Ad-

K38A) and photo-activated GFP (Ad-PAGFP) as control were previously described (21). An adenovirus expressing the DRP1 mutant, S656A DRP1 (S636 in human DRP1), in which the serine residue was substituted by alanine, was obtained from Dr. Stefan Strack, University of Iowa, IA (15). β-Cells were treated according to the experimental protocol 3 d after infection at MOI 250. Expression was verified by Western blotting for total DRP1. Baculovirus expressing ER-*Gfp* was purchased from Invitrogen.

Confocal microscopy

Primary mouse and human islet cells and INS-1E β-cells were imaged with a 63x oil objective on a Zeiss LSM 710 confocal microscope equipped with an incubator (Zeiss, Oberkochen, Germany). ER and mitochondrial morphology were analyzed using Metamorph software (Molecular Devices, Sunnyvale, CA). Image analysis was performed on multiple consecutive 0.2 μM confocal sections, allowing definitive distinction between cells with continuous thin ER structures (defined as tubular ER) or with large cisternae-like structures (expanded ER). To quantify ER expansion we analyzed ER images of cells expressing ER-*Gfp*. Images were thresholded above background and the average diameter of tubular ER in control cells calculated and used as a reference. ER was defined as expanded when > 50% of the ER showed diameter at least three times greater than the reference. These criteria were validated in INS-1E cells and MEFs treated with the ER stressor thapsigargin that was used as a positive control. The images were analyzed by two independent observers; one of them was blinded to treatment conditions. ER imaging criteria were uniformly used in all experiments, allowing objective assessment of ER morphology under the different treatment conditions. Mitochondria morphology was analyzed and designated tubular or fragmented, as previously described (21, 22). Scatter-plot graphs of GFP-DRP1 vs. turquoise-ER were obtained with ImageJ software (NIH, Bethesda, MD) and overlap coefficients and correlation R by Zen software (Zeiss).

Super-resolution imaging

For super-resolution imaging we used a Nikon N-SIM confocal microscope that allows a resolution of 85 nm (Nikon, Tokyo, Japan). INS-1E β-cells were seeded on Ibidi 35 mm plates (Munich, Germany), with a 1.523 refractive index glass coverslip bottom (170 +/- 10 μm thickness). Prior to imaging the point-spread function was visualized with 100 nm fluorescence beads in order to adjust the correction ring of the objective to the coverslip thickness. A 100x oil objective with NA value of 1.49 was used. The raw data was examined carefully, and the optical grid pattern was clearly visible in all sets of images that were used. Images were reconstructed with NIS-Elements software (Nikon).

Electron microscopy

Cultured mouse islet cells or INS-1E β-cells were fixed using a solution of cold 2.5% glutaraldehyde, 2% formaldehyde and 0.1 mol/l acodylic acid, cut into ultrathin sections and imaged with a transmission electron microscope (EM) (Tecnai 12 TEM, Phillips, Eindhoven, the Netherlands).

Isolation of ER and mitochondria

Cells were broken by osmotic swelling and Dounce homogenization, and remaining intact cells and nuclei spun down at 1000 g for 10 min. The supernatant was centrifuged at 12000 g for 15 min to obtain a mitochondrial pellet. The postmitochondrial supernatant was centrifuged at 100000 g to obtain an ER pellet. ER enrichment was verified with a kit measuring the ER resident NADPH-Cytochrome C reductase activity (Sigma) and by Western blotting for the ER resident IRE1α. Mitochondrial enrichment was verified by Western blotting for the mitochondrial proteins Complex II and cytochrome C. The cytosol marker chosen was GAPDH.

AMPK-DRP1 phosphorylation assay

Phosphorylation of human DRP1 by AMPK was tested using human recombinant Drp1 (Novus, Littleton, CO) and human AMPKα1β1γ1 (GenScript, Piscataway, NJ) using an HTRF Transcreener ADP kit (Cisbio, Bagnols/Ceze, France) and the known AMPK substrate SAMS as positive control. Data was recorded by Pherastar Plus (BMG LABTECH, Ortenberg, Germany). The experiment was performed at the Genscript facility.

Western blotting

Protein expression in INS-1E β-cells *was* assessed by standard Western blotting using antibodies against IRE1α, phosphorylated PERK, phosphorylated eIF2α, phosphorylated JNK (Thr183/Tyr185), total and phosphorylated (S79) ACC, total and phosphorylated (Thr172) AMPK, total and phosphorylated (S616/637) Drp1, cytochrome C, HSP90 and caspase-3 (Cell Signaling, Beverly, MA); GAPDH, CHOP (Santa Cruz Biotechnology, Santa Cruz, CA); and Complex II (Mitosciences, Eugene, OR). X-ray film densitometry was used for quantification (ImageMaster VDS-CL, Amersham Pharmacia Biotech, Amersham, UK).

Quantitative real-time RT-PCR

RNA was extracted from INS-1E cells using Bio Tri RNA (Biolab, Jerusalem, Israel). Samples of 1 μg total

RNA were reverse-transcribed using Moloney murine leukemia virus reverse transcriptase (Promega, Madison, WI). Quantitative real time RT-PCR (qPCR) for spliced *Xbp1* was performed with StepOnePlus™ Real-Time PCR System, using the Power SYBR® Green Gene Expression Assay (Applied Biosystems, Foster City, CA). All samples were analyzed in triplicate; GAPDH (Applied Biosystems) was used as internal control.

Apoptosis ELISA assay

INS-1E cells plated in 96-well plates were treated and then lysed and oligonucleosomes in the cytosol, indicative of apoptosis-induced DNA degradation, quantified using the Cell Death Detection ELISA^{PLUS} kit (Roche Diagnostics, Mannheim, Germany) according to the manufacturer's instructions.

Oxygen consumption

Oxygen consumption was measured in INS-1E cells in V7 culture plates in an XF24 respirometer (Seahorse Bioscience, Billerica, MA). One-hour prior to measurements, culture medium was replaced with assay medium containing 3 mmol/l glucose, 0.8 mmol/l Mg^{2+}, 1.8 mmol/l Ca^{2+}, 143 mmol/l NaCl, 5.4 mmol/l KCl, 0.91 mmol/l NaH2PO4 and 15 mg/ml phenol red (Seahorse Bioscience). Measurements were recorded before and consecutively after stimulation with 20 mmol/l glucose and 1 μmol/l FCCP.

Insulin and proinsulin content and secretion

Islets were recovered overnight and then groups of islets were treated with and without 0.5 mmol/l palmitate and/or 1 mmol/l AICAR for 16 h. Insulin response to glucose was evaluated by static incubation of islets in four-chamber culture plates (Nunclon δ Multidishes; Nunc A/S, Roskilde, Denmark) with 20 islets/chamber in quadriplicates. Batches of islets were preincubated for 60 min in RPMI 1640 containing 3.3 mmol/l glucose and then were consecutively incubated at 3.3 mmol/l and 16.7 mmol/l glucose for 1 h at 37°C in 1 ml of modified Krebs-Ringer bicarbonate buffer containing 20 mmol/l HEPES and 0.25% BSA (KRBH-BSA). Medium was collected at the end of the basal (3.3 mmol/l glucose) and stimulated (16.7 mmol/l glucose) incubations, centrifuged, and frozen at –20°C pending insulin assay. Islet insulin and proinsulin content were determined by RIA and ELISA, respectively, in extracts of islets subjected to repeated freeze-thaw cycles in 1.5-ml microfuge tubes containing 450 μl 0.1% BSA in 0.1 N HCl. Mouse insulin immunoreactivity in islet extracts and in the medium was determined using a rat RIA kit (Millipore, Bedford, MA) and islet proinsulin content using an ELISA kit (Mercodia, Uppsala, Sweden). The antiserum used for proinsulin measurement does not cross-react with insulin or C-peptide.

Statistical analysis

Data are given as means +/- SEM. The differences between multiple groups means were analyzed by one-way ANOVA with post hoc Bonferroni corrected two-tailed *t* test. Two-tailed unpaired Student's *t* test was used to compare differences between two groups. A *P* value of less than 0.05 was considered significant.

Results

Induction of ER expansion by ER stressors in mouse islets and clonal β-cells

We employed several imaging techniques to study ER morphology in ER stress. Primary mouse β-cells were infected with a baculovirus expressing *ER-Gfp* and then treated with palmitate or the SERCA inhibitor thapsigargin for different periods of time followed by confocal microscopy and electron microscopy (EM) analysis. In nonstressed β-cells, ER morphology was mainly tubular; treatment with palmitate (0.5 mmol/l) or thapsigargin (300 nmol/l) for 6 h induced marked ER expansion (Figure 1). Electron microscopy (EM), super-resolution confocal microscopy and detailed z-stack imaging of sections spanning 1–2 μm showed that under stressful conditions the fine tubular structure of ER was replaced by sack-like cisternae (Figure 1A-C). At this time point, 60% and 45% of cells treated with palmitate or thapsigargin, respectively, acquired ER cisternae shape (Figure 1D). Similar findings were observed in INS-1E cells labeled with eYFP-ER and by EM (Supplemental Figure 1). ER enlargement appeared in ~70% of INS-1E cells already after 3 h of palmitate or thapsigargin treatment; thereafter the ER appeared fragmented in a minority of the cells, most probably secondary to apoptosis (Supplemental Figure 1). The poly-unsaturated FFA oleate and the nonmetabolizable FFA methylpalmitate did not elicit morphological changes (not shown). Of note, palmitate-induced ER expansion appeared prior to the development of apoptosis and was reversible following removal of palmitate from the culture medium (Supplemental Figure 2A). By contrast, the morphological changes induced by thapsigargin were not reversed, probably because thapsigargin binding to SERCA is irreversible. ER changes were similar in mouse β-cells and in INS-1E cells; therefore, the latter were used for further mechanistic studies.

ER stress and regulation of ER morphology

ER expansion peaked at 3–6 h of palmitate treatment. We therefore analyzed UPR activity at these time points. As expected, treatment with palmitate stimulated the UPR, evident by increased eIF2α phosphorylation, CHOP expression, spliced *Xbp1*, as well as JNK and cJUN phosphorylation (Figure 2A). We have previously shown that high glucose amplifies palmitate-induced ER stress (glucolipotoxicity) (23); however, treatment with high glucose alone or adding high glucose to palmitate did not modify ER morphology (Supplemental Figure 2B). To further study whether ER stress per se causes ER expansion, we treated β-cells with a cytokine cocktail (IL-1β+TNFα+IFNγ) or tunicamycin, which induces ER stress by inhibiting N-linked protein glycosylation. Although as expected cytokines and tunicamycin stimulated different parameters of cellular stress (Supplemental Figure 3 and Figure 2B), they did not induce any ER expansion. At 24 h, cytokines and tunicamycin induced ER fragmentation, most probably reflecting apoptotic cells (Figure 2C-D; cytokines effects not shown). These findings imply that modulation of ER stress per se does not necessarily entail modified ER morphology.

IRE1α has been implicated in the regulation of ER morphology (24). To study its role in stressed cells, we used mouse embryonic fibroblasts (MEFs) derived from *IRE1α* and *Xbp1* knock out mice. These contained fewer flat cisternae-like structures than wild-type (WT) MEFs (Figure 2E, F), suggesting that spliced Xbp1 regulates ER morphology in nonstressed cells. Similar to β-cells, palmitate induced ER expansion in WT MEFs; strikingly, the morphological response to palmitate in *IRE1α* and *Xbp1* KO cells was similar to that in WT cells (Figure 2E, G). Collectively, these findings indicate that stimulation of the UPR is not sufficient, nor necessary, for stress-induced ER enlargement.

DRP1 is an ER resident and regulates ER morphology in stressed β-cells

Dynamin-related-protein 1 (DRP1) is a mitochondrial fission protein; its inhibition prevents palmitate-induced

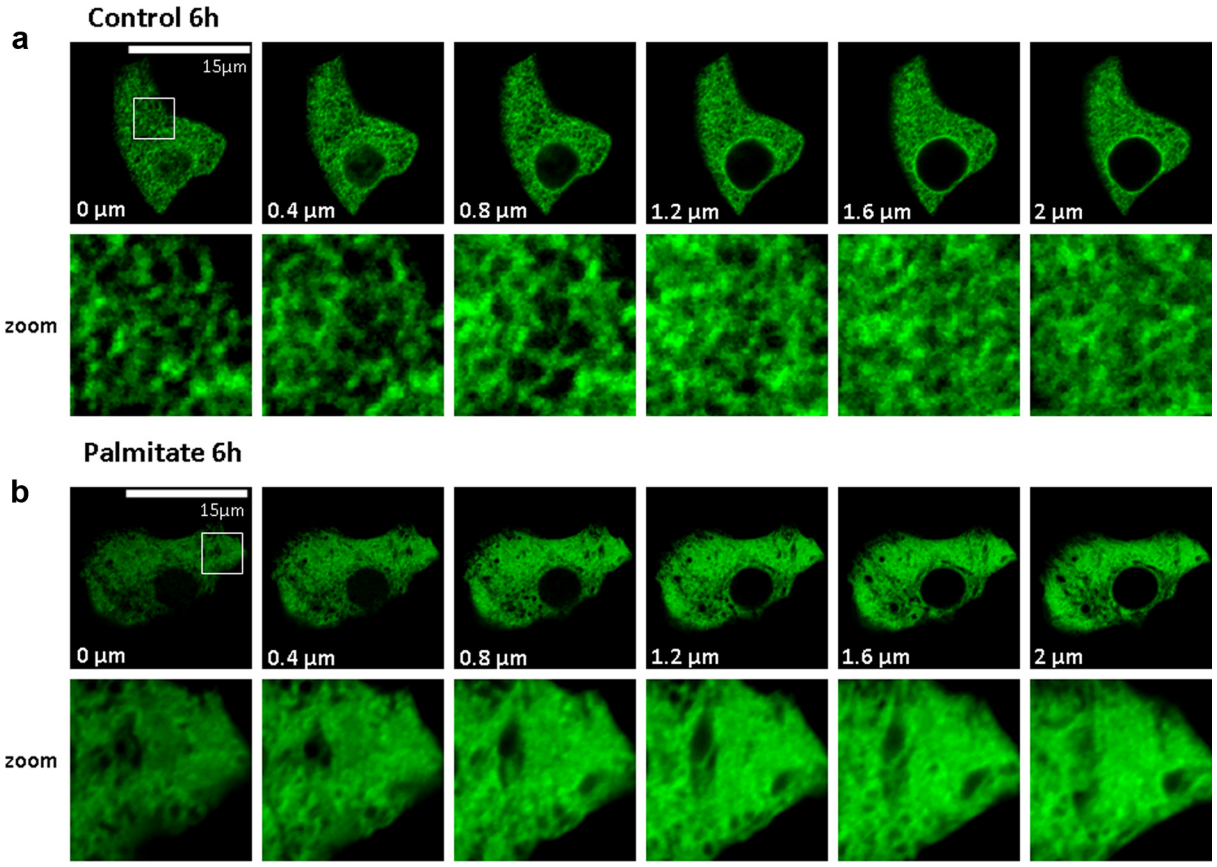

FIGURE 1A. Effects of ER stressors on ER morphology in primary β-cells. Primary mouse β-cells expressing GFP-ER were treated at 11.1 mmol/l glucose with 0.5 mmol/l palmitate or 300 nmol/l thapsigargin for 6 and 24 h. ER morphology was analyzed by confocal microscopy (A-C). Distance between sections in the z-stack confocal imaging is indicated (μm). Note that cisternal structures are continuous throughout several sections under palmitate and thapsigargin treatment. D) Quantification of the number of primary mouse β-cells with expanded (cisternal) ER morphology (C=control, P=palmitate, T=thapsigargin). Results are means ± SEM of four (6 h) and six (24 h) separate experiments analyzing 20–40 cells imaged per treatment; * $P < .05$ and ** $P < .01$. E) Electron microscopy images of primary mouse β-cells. Yellow square indicates zoom area. Arrows point to ribosomes on ER membrane. Size bar = 500 nm.

mitochondrial fission in β-cells (22). DRP1 is recruited from a cytosolic pool to mitochondrial fission sites, which are often present in areas of ER-mitochondria interactions (25); therefore we studied the intracellular localization of DRP1 and its role in regulating ER morphology in stressed β-cells. First, we labeled INS-1E β-cells with GFP-DRP1, the ER marker turquoise-ER and the mitochondrial dye TMRE. As expected, we observed intense GFP-DRP1 punctae on mitochondria, indicative of mitochondrial fission sites (Figure 3A). In addition, there was considerable colocalization of the DRP1-GFP and the ER marker, indicating that DRP1 is also localized to the ER (Figure 3A, B). The overlap and correlation coefficients were 0.83 ± 0.02 and 0.76 ± 0.03, respectively. To confirm this, we performed subcellular fractionation and isolated cytosol, mitochondria and ER from nontransfected INS-1E cells (Figure 3B). The purity of the fractions was confirmed by Western blot for specific cytosol and mitochondria markers and by analyzing cytochrome C reductase activity for ER purity (Figure 3C, D). DRP1 was

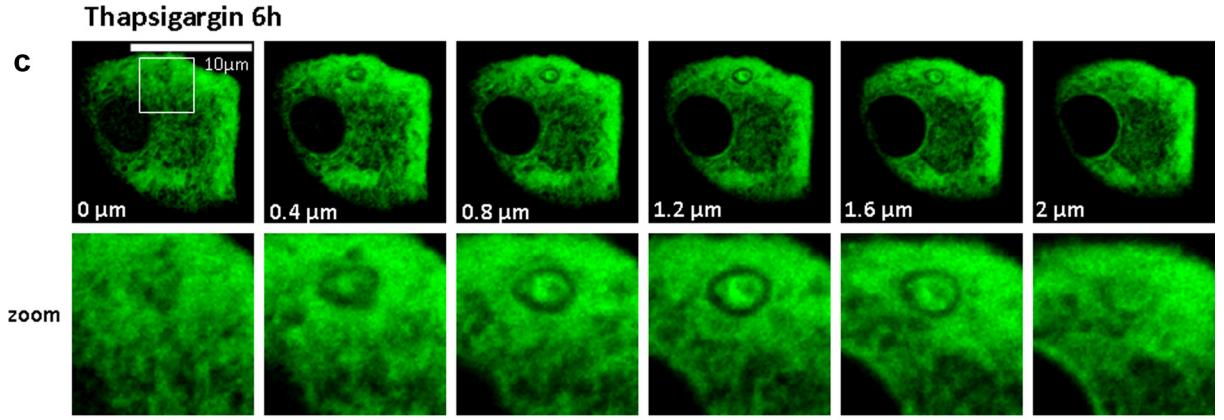

FIGURE 1B.

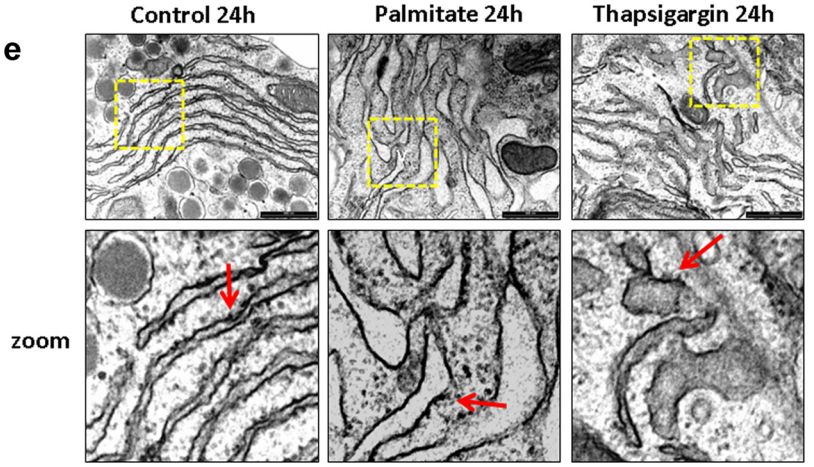

FIGURE 1C.

expressed both in the cytoplasm and in the ER and to a much lesser extent in mitochondria. Thus, we conclude that DRP1 is a *bona fide* ER resident in β-cells.

Next, we inhibited DRP1 action by adenoviral expression of DRP1 DN (Ad-K38A) (Figure 4). Expression of DRP1 DN did not affect the morphology of the ER while it induced mitochondrial hyperfusion as expected (Figure 4B), though mitochondrial function reflected by oxygen consumption was not affected (not shown), suggesting that DRP1 has a minor role in the regulation of ER morphology and mitochondrial function in nonstressed β-cells. By contrast, DRP1 DN markedly reduced ER expansion, as well as mitochondrial fragmentation, induced by palmitate (Figure 4B, D). DRP1 was present in mito-

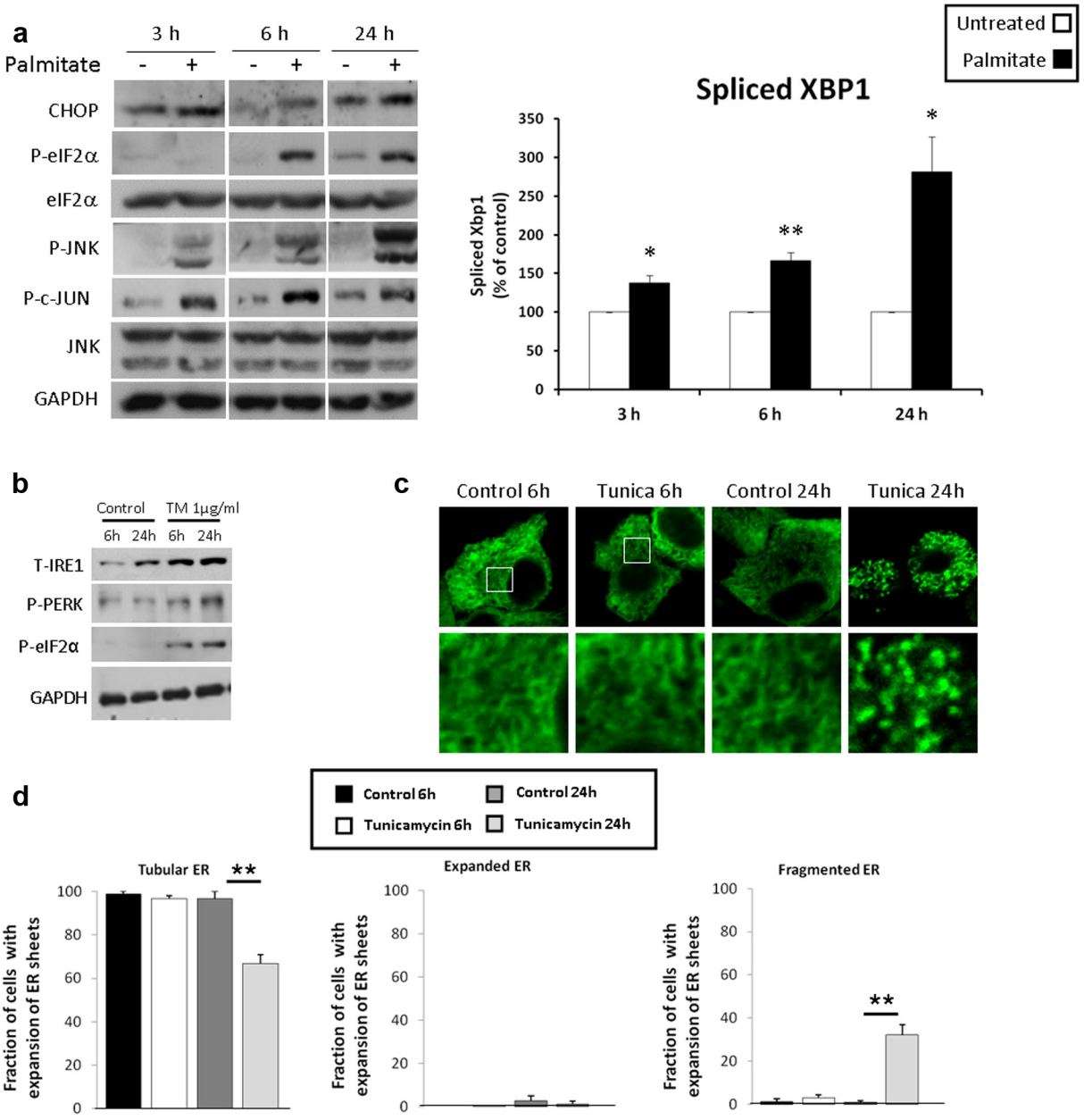

FIGURE 2A. Effect of ER stress on ER cisternal expansion. A) Effect of palmitate on UPR activity. INS-1E β-cells were treated at 11.1 mmol/l glucose with control media or 0.5 mmol/l palmitate for different periods of time. CHOP expression, eIF2α, JNK, and c-JUN phosphorylation analyzed by Western blot (n = 4–9). Spliced Xbp1 was analyzed by real time PCR (n = 5–6). B-D) Effect of tunicamycin on ER morphology. INS-1E β-cells expressing GFP-ER were treated at 11.1 mmol/l glucose without and with 1 μg/ml tunicamycin for 6 and 24 h followed by confocal microscope analysis of ER morphology. B) Tunicamycin effects on the expression and phosphorylation of different UPR markers. C) Representative confocal imaging of the ER of tunicamycin-treated β-cells. D) The percentage of cells with tubular, expanded or fragmented ER is shown. Results are expressed as means ± SEM of 3–5 separate experiments analyzing 46–76 cells and compared to control cells at the same time point. E) Confocal microscopy of wild-type (WT), *IRE1α* or *Xbp1* deficient mouse embryonic fibroblasts (MEFs) expressing eYFP-ER and treated with control media or 0.5 mmol/l palmitate for 6h. White square indicates zoom area. F, G) Quantification of ER morphology in untreated and palmitate-treated MEFs. Results are expressed as means ± SEM of 5–6 separate experiments analyzing 15–46 cells per treatment. * $P < .05$ and ** $P < .01$.

chondrial fission sites (Figure 4E) and the number of GFP-DRP1 punctae per cell decreased in cells where mitochondria were fragmented (Figure 4F). Collectively, these findings suggest that DRP1 mediates palmitate-induced ER expansion and mitochondrial fragmentation, followed by dissociation from mitochondrial fission complexes and departure from these sites.

Regulation of DRP1 phosphorylation by β-cell stressors and AMPK

DRP1 function is regulated by several post-translational modifications including phosphorylation (26). Phosphorylation at S616 is associated with increased activity of DRP1 (profission), while phosphorylation at S637 is linked to reduced activity (antifission) (27). This was confirmed in β-cells by treatment of INS-1E cells with the mitochondrial uncoupler FCCP which induces mitochondrial fragmentation (Figure 5A). As expected, FCCP markedly decreased S637 phosphorylation (Figure 5B). Palmitate mildly decreased S616 and S637 phosphorylation (Figure 5C-D), which may suggest that FFA stimulation of DRP1 is not mediated via modulation of DRP1 phosphorylation. By contrast, high glucose and cytokines that did not expand the ER increased S637 phosphorylation and S637/S616 phosphorylation ratio (Supplemental Figure 3). Hence, we hypothesized that DRP1 S637 regulates ER morphology; its phosphorylation preventing ER expansion. To test this hypothesis we attempted to modulate DRP1 S637 phosphorylation and studied the impact on palmitate-induced ER expansion. AMPK plays an important role in the regulation of nutrient stress through its kinase activity (28), thus we hypothesized that AMPK may affect DRP1 phosphorylation, thereby modulating ER morphology. Pharmacological activation of AMPK by AICAR increased phosphorylation at S637 both in the absence and presence of palmitate, whereas S616 phosphorylation, and total DRP1 expression were unaffected (Figure 5C, D). We further studied whether AMPK directly phosphorylates the DRP1 S637 site by an in vitro phosphorylation assay using human AMPK$\alpha1\beta1\gamma1$ and DRP1 proteins. The AMPK substrate SAMS was used as a positive control and showed robust phosphorylation by AMPK (Figure 5E). In contrast, DRP1 was not phosphorylated by AMPK in vitro, indicating that its cellular effect on S637 phosphorylation is indirect.

AMPK activation prevents palmitate-induced ER enlargement in β-cells

We further examined the effects of the AMPK activators AICAR and metformin on ER changes induced by

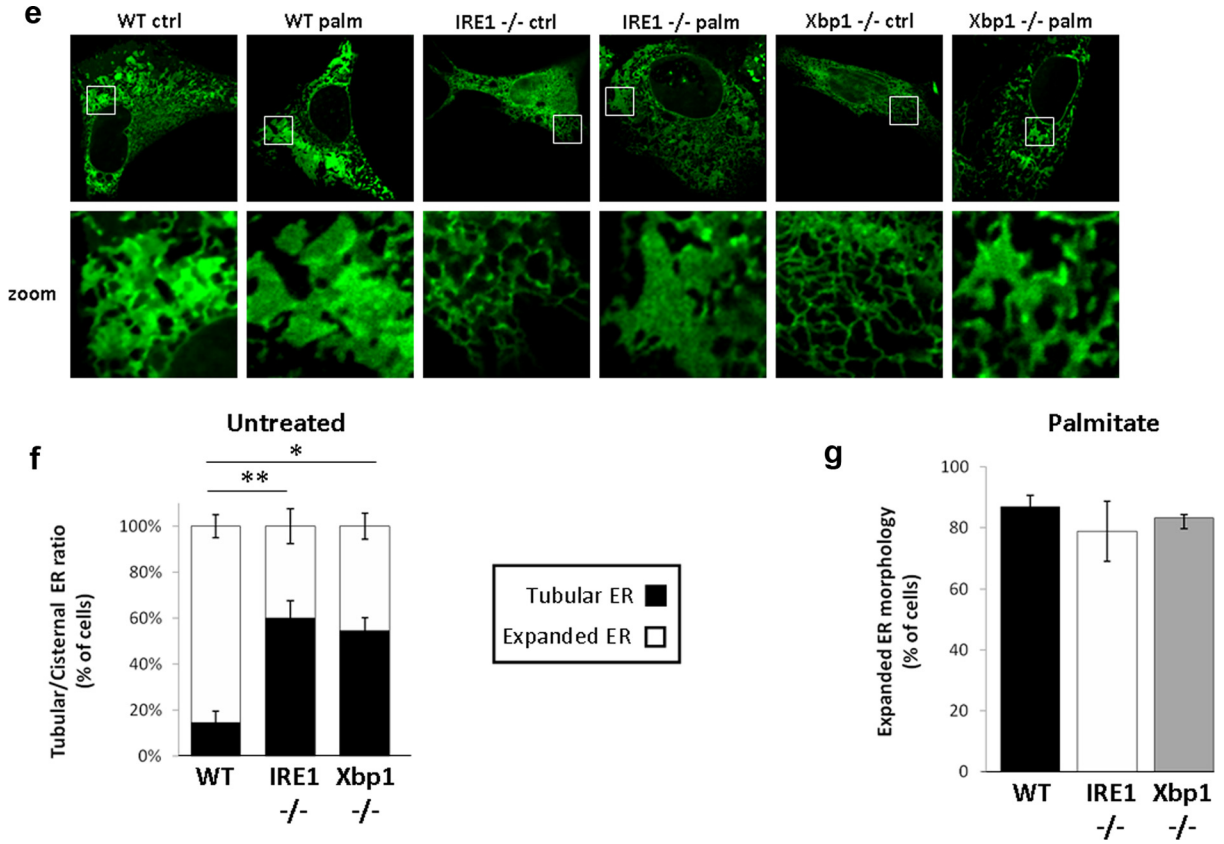

FIGURE 2B.

palmitate in INS-1E cells and human islets. Both drugs markedly decreased palmitate-induced ER enlargement (Figure 6). To exclude off-target effects of AICAR, we used an AMPK dominant negative (DN) construct (Figure 6F, G). Expressing AMPK DN in β-cells abolished the rescue by AICAR of palmitate-induced ER enlargement, indicating that the AICAR effect is indeed mediated via AMPK. Next, we studied whether AMPK activation by AICAR rescued ER and mitochondria morphology by DRP1 phosphorylation. We transduced β-cells with the rat DRP1 phosphorylation mutant (GFP-DRP1 S656A). The rat S656 parallels the S637 site in man (27). Strikingly, as compared to wild type GFP-DRP1, GFP-DRP1 S656A attenuated the rescue effect of AMPK on ER and mitochondria morphology, although the effect on the mitochondria was not statistically significant (Figure 6H-I). In summary, AMPK phosphorylation of DRP1 at S637 in man/S656 in rat mediates its effects on ER and mitochondria morphology.

AMPK regulation of ER morphology in vivo was studied in mice with conditional deletion of the AMPK upstream regulator *LKB1* in β-cells; these β-cells express exceedingly low AMPK activity (29, 30). Electron microscopy of LKB1 null β-cells revealed marked enlargement of the ER (Figure 6J), suggesting that LKB1/AMPK regulates ER morphology in vivo even in the absence of exogenous stress. Stimulation of AMPK impacts several metabolic pathways that may affect ER configuration. We tested this by using different pharmacological modulators of AMPK downstream targets and of FFA metabolism, including fumonisin B1 (ceramide synthase inhibitor), simvastatin (HMG-CoA reductase inhibitor), rapamycin (mTORC1 inhibitor) and etomoxir (CPT1 inhibitor); however, none of these compounds modified the palmitate or AICAR effects on ER morphology.

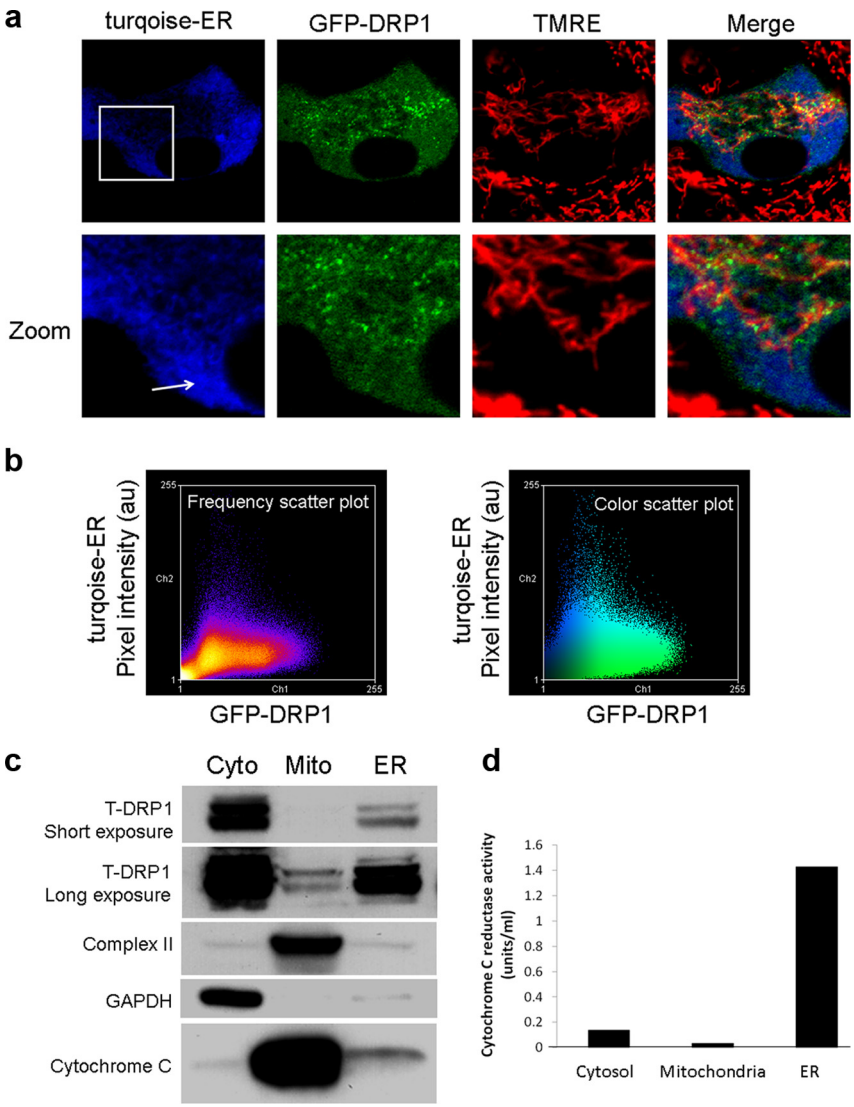

FIGURE 3. Intracellular localization of DRP1. A) Colocalization of DRP1 and ER in INS-1E β-cells. DRP1 and ER are visualized by expression of GFP-DRP1 and turquoise-ER and mitochondria by staining with the dye TMRE. B) Scatter plots of GFP-DRP1 vs. turquoise-ER (of images in [A]). C) Subcellular localization of DRP1 by Western blotting. Cytosol, mitochondria and ER were isolated from INS-1E β-cells, followed by Western blotting for DRP1; GAPDH used as cytosol marker and Complex II and cytochrome C for mitochondria. D) Cytochrome C reductase activity in cytosolic, mitochondrial and ER fractions.

Impact of AMPK activation on stressed β-cell function

In β-cells, proper function of the ER is essential for proinsulin transport to the Golgi and effective processing and channeling to the secretory pathway. We therefore performed single-cell analyses of proinsulin retention in the ER in β-cells that were transfected with GFP-proinsulin and the ER marker RFP-ER, then treated with palmitate and/or AICAR for 6 h. In palmitate-treated β-cells, the retention of proinsulin-GFP in the ER was increased in cells presenting ER expansion, evident by greater colocalization of GFP-proinsulin and RFP-ER compared to cells lacking ER expansion (Figure 7A). Treatment with AICAR decreased the number of cells with ER expansion, and resulted in reduced proinsulin-GFP retention in the ER. Finally, we found that

palmitate decreased islet insulin content and increased the proinsulin/insulin ratio in mouse islet extracts, whereas AICAR prevented these changes (Figure 7B, C). Treatment with palmitate significantly increased basal mitochondrial respiration and insulin secretion and decreased glucose-stimulated insulin secretion (Supplemental Figure 4). By contrast, AICAR inhibited basal oxygen consumption in control and palmitate-treated cells and prevented the palmitate effects on insulin secretion. Despite the suppressive effect of AICAR on insulin secretion, the response to glucose was augmented by 2-fold (Figure 7D and Supplemental Figure 4). Insulin secretion of islets

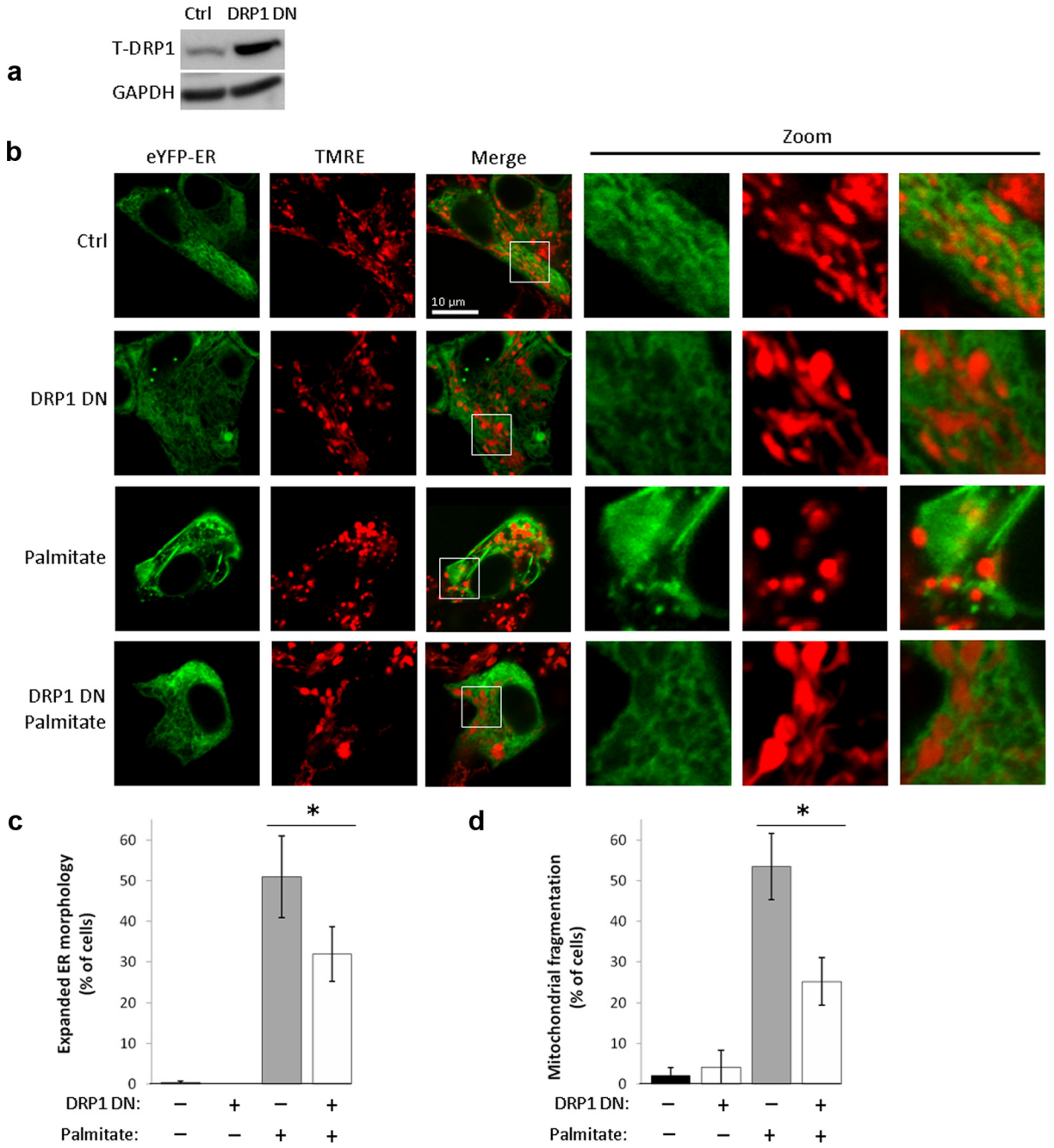

FIGURE 4A. Effect of DRP1 inhibition on palmitate-induced ER expansion and mitochondrial fragmentation. INS-1E β-cells were transduced with an adenovirus vector expressing dominant negative (DN) DRP1 or with photoactivatable GFP (PAGFP) used as control (Ctrl). A) DRP1 expression analyzed by Western blotting. B) INS-1E β-cells expressing eYFP-ER were treated at 11.1 mmol/l glucose with control media or 0.5 mmol/l palmitate for 6 h and then stained with the mitochondrial dye TMRE. White square indicates zoom area. C, D) Quantification of palmitate-induced ER expansion and mitochondrial fragmentation in INS-1E β-cells expressing DRP1 DN and in control cells. Results are expressed as means ± SEM of 5–6 separate experiments analyzing 11–66 cells per treatment. E) DRP1 is present in palmitate-induced mitochondrial fission sites. Cells expressing GFP-DRP1 and stained with the mitochondrial dye TMRE. F) Quantification of GFP-DRP1 punctae on mitochondria. Results are means ± SEM of 3 separate experiments analyzing 6–23 cells. * $P < .05$, ** $P < .01$.

treated with palmitate and AICAR together was similar to that of the AICAR alone group. FCCP-stimulated maximal respiration was not affected by palmitate and/or AICAR (Supplemental Figure 4), thus their effects on insulin secretion cannot be attributed to modulation of mitochondrial metabolic capacity. In summary, palmitate treatment impaired, whereas stimulation of AMPK ameliorated palmitate-induced β-cell dysfunction.

Impact of stimulating AMPK on mitochondrial fragmentation and apoptosis in palmitate-stressed β-cells

Since AMPK activation inhibited DRP1, we studied its effect on mitochondrial morphology and function. AICAR did not affect mitochondrial morphology in control cells, but markedly decreased mitochondrial fragmentation induced by palmitate (Figure 8A, B). We further examined the effect of AMPK activation on apoptosis. Intriguingly, AICAR alone increased cleaved caspase-3, measured by Western blotting, and nucleosome content, measured by ELISA (Figure 7C, D). However, when added to palmitate, AICAR significantly reduced β-cell apoptosis measured by these parameters (Figure 8C, D).

Discussion

In this study we describe a novel signaling pathway that we believe plays a central role in transmitting the effect of increased FFA on β-cell dysfunction. We found that the mitochondrial fission protein DRP1, an ER resident in β-cells, is controlled by AMPK, and is implicated in the ER shape and function modifications that occur under lipotoxic conditions.

Organelle morphology and interorganelle interactions may have robust effects on cellular function and survival. The current study sheds new light on the regulation of ER

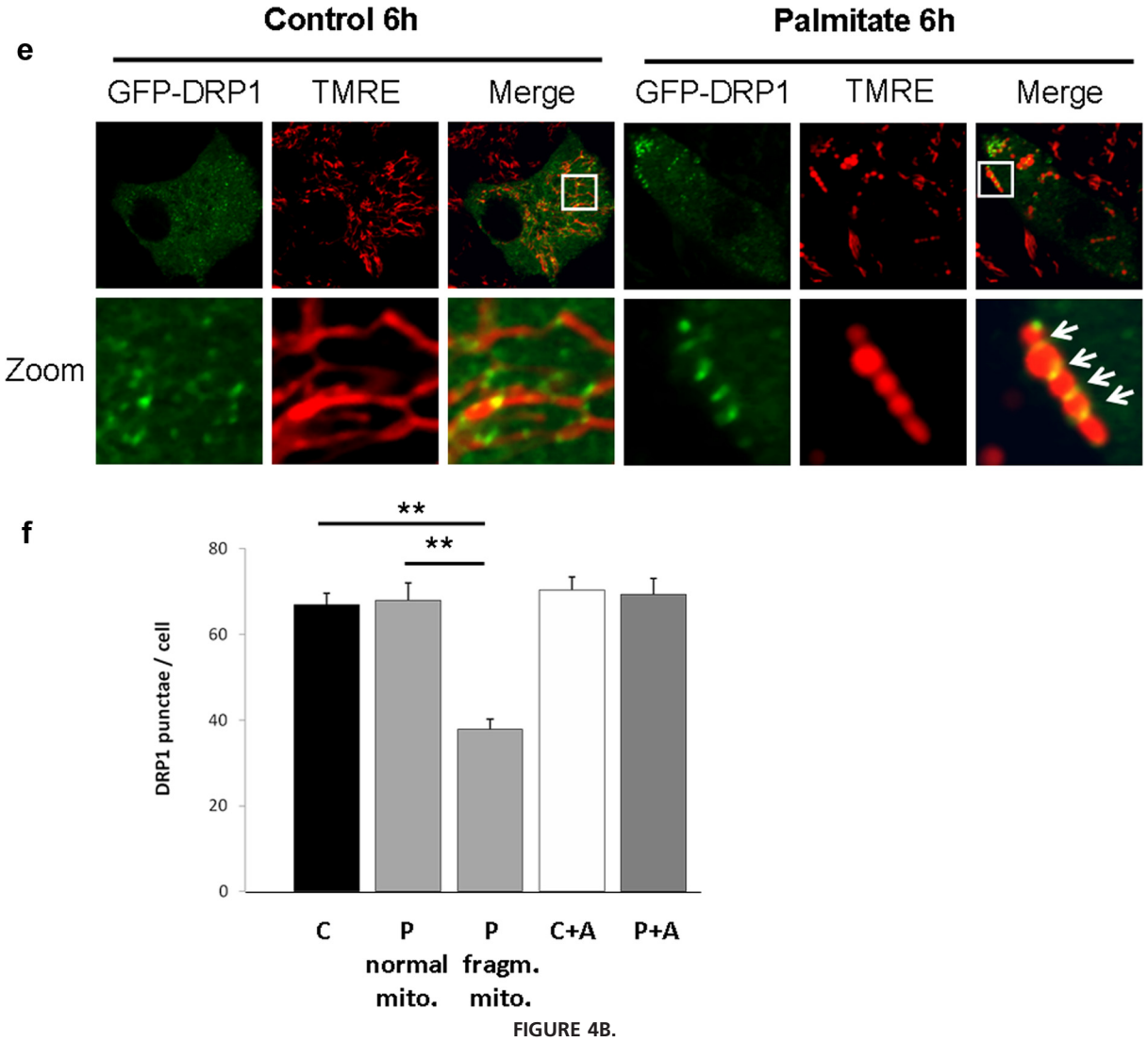

FIGURE 4B.

morphology in metabolic stress and its impact on β-cell function. Previous studies in other mammalian cells and yeast showed that ER stress may induce varying morphological changes in the ER (31–33). Enlargement of the ER was reported in β-cells exposed to palmitate, as well as to other inducers of ER stress (34, 35). However, most studies lacked comprehensive assessment of ER morphology. In the present study, detailed qualitative and quantitative analyses of ER morphology showed that in nonstressed β-cells the ER consists mainly of narrow and long tubular structures. Stressing β-cells or MEFs with palmitate or thapsigargin transformed the tubular ER into larger sack-like cisternal structures. It could be expected that stress-induced ER expansion is mediated via the UPR; however, several lines of evidence indicate that this is not the case. High glucose and cytokines that are involved in diabetes pathophysiology and activate β-cell stress did not expand the ER. Also tunicamycin, a potent inducer of ER stress and the UPR, did not expand the ER. Finally, IRE1α and Xbp1 deficiency did not affect the alteration of ER morphology by palmitate or thapsigargin.

Previous studies showed that IRE1α regulates ER biogenesis and expansion in various non-β-cell types (36–38). This was mediated via the endoribonuclease activity

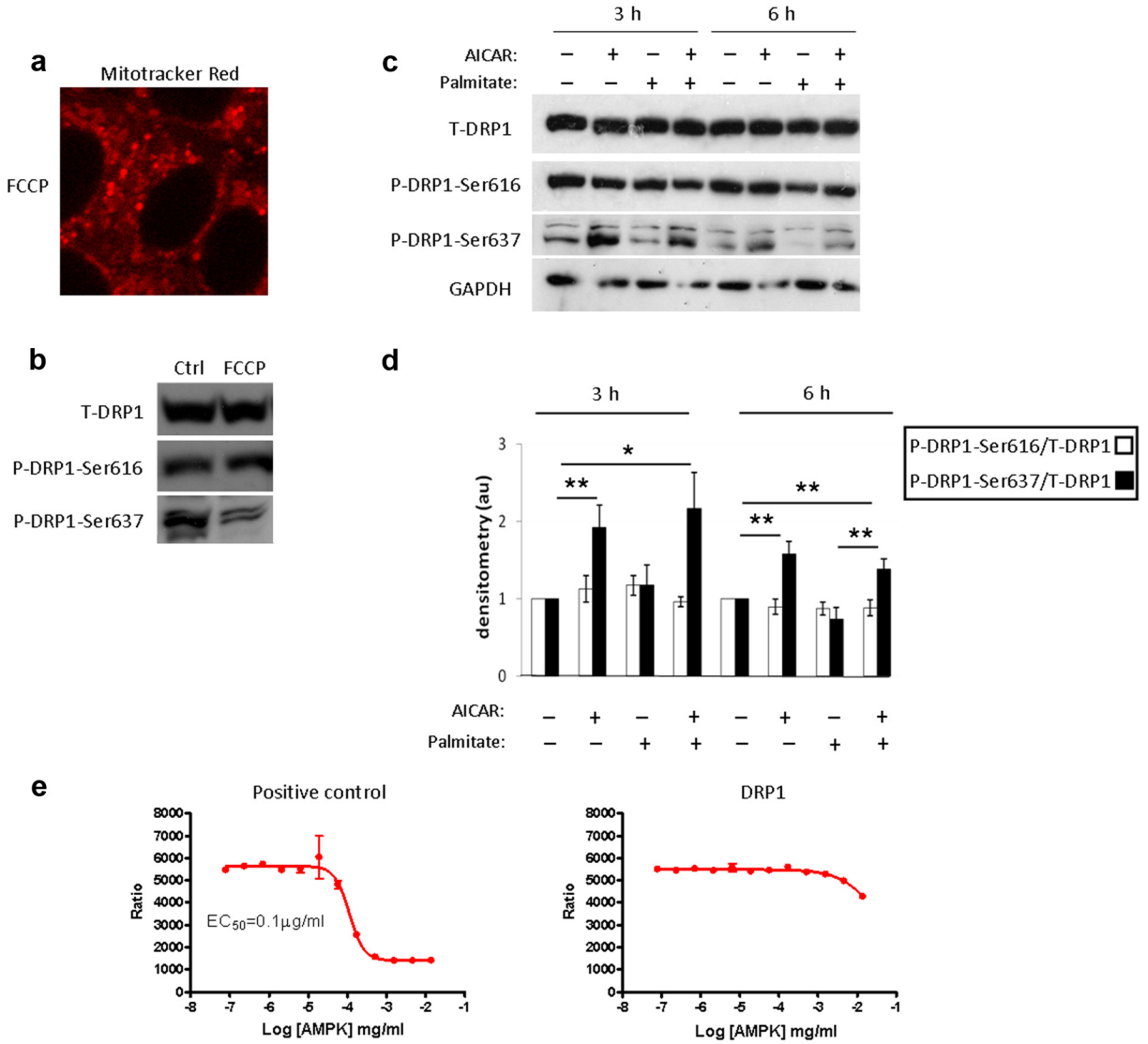

FIGURE 5. AMPK regulation of DRP1 phosphorylation. A) Mitochondrial fragmentation induced by FCCP. INS-1E β-cells stained with Mitotracker red. B) Effect of mitochondrial fragmentation by FCCP on DRP1 phosphorylation. INS-1E β-cells were treated with FCCP for 60 min followed by Western blotting for total DRP1 and DRP1 S616 and S637 phosphorylation. C) AMPK activation by AICAR increases DRP1 S637 phosphorylation. INS-1E β-cells were treated at 11.1 mmol/l glucose with control medium or 0.5 mmol/l palmitate with and without 1 mmol/l AICAR for different periods of time, followed by Western blotting for total and phospho-S616 and S637 DRP1. D) Quantification of S616 and S637 DRP1 phosphorylation corrected for total DRP1. Results were then normalized to untreated control cells at each time point. Results are means ± SEM of 8 separate experiments. E) In vitro protein phosphorylation assay analyzing phosphorylation of human DRP1 by AMPKα1β1γ1; SAMS peptide used as a positive control. * $P < .05$, ** $P < .01$.

of IRE1α and its product spliced Xbp1 (36, 39). Consistent with these findings, we found that MEFs lacking IRE1α or Xbp1 contained fewer cisternae-like structures, suggesting that in nonstressed cells, spliced Xbp1 participates in the regulation of ER morphology. In yeast, the IRE1α orthologue Ino2/4 regulates ER expansion in response to stress (33); however we could not confirm this finding in mammalian cells; indeed, the ER in Xbp1-deficient cells reacted to stress identically as in WT cells. Thus, while we cannot exclude UPR implication in the

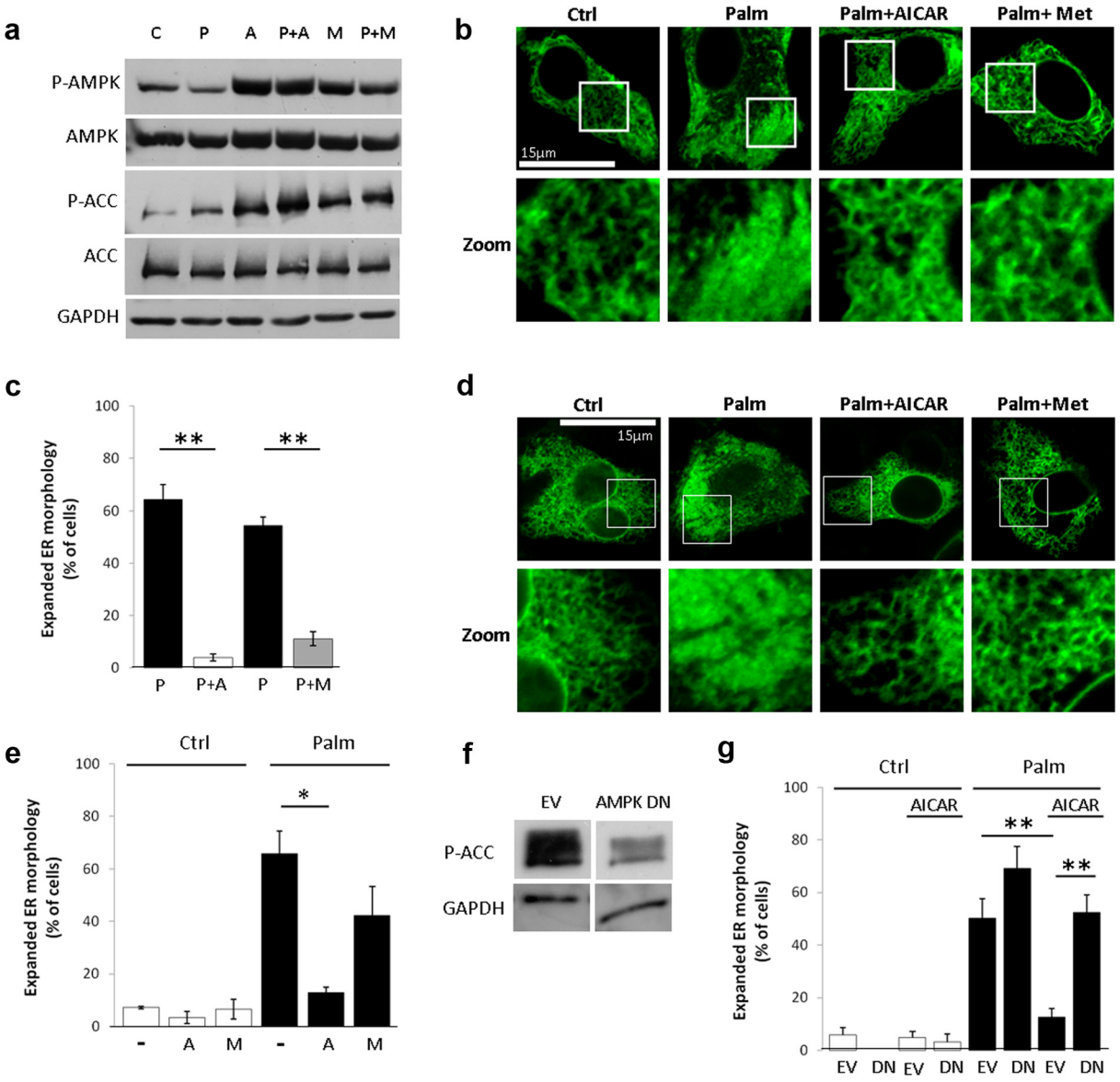

FIGURE 6A. Effect of AMPK activation on palmitate-induced ER expansion. A) AMPK activation by AICAR and metformin. INS-1E β-cells were treated as indicated at 11.1 mmol/l glucose for 6 h (C=control, P=palmitate (0.5 mmol/l), A=AICAR (1 mmol/l), M=metformin (1 mmol/l). AMPK activity analyzed by Western blotting for phosphorylated (Thr172) AMPK and phosphorylated (Ser79) acetyl-CoA carboxylase (ACC). B-E) Effect of AMPK activation on palmitate-induced ER expansion in INS-1E β-cells (B, C) and human islets (D, E). INS-1E β-cells and human islets expressing eYFP-ER were treated as indicated incubated at 11.1 mmol/l glucose for 6 h followed by confocal microscopy (Ctrl=control, Palm=palmitate, A=AICAR, Met=metformin). White square indicates zoom area. C, E) Quantification of ER expansion in INS-1E β-cells and human islets. Results are means ± SEM of 6 separate experiments analyzing at least 40 cells per treatment (C), and of 3–4 separate experiments analyzing at least 30 cells per treatment (E). F) Effect of AMPK dominant negative on AMPK activity. INS-1E β-cells were transduced with an AMPK dominant negative adenoviral vector followed by Western blotting for total and phospho-ACC (EV=empty vector, DN=dominant negative). G) Quantification of ER expansion in INS-1E β-cells transduced with empty vector (EV) or AMPK dominant negative (DN) and treated with or without palmitate and/or AICAR at 11.1 mmol/l glucose for 6 h. Results are means ± SEM of 3–4 separate experiments analyzing at least 40 cells per treatment. H-I) Quantification of ER and mitochondrial morphology in cells expressing wild type and phosphorylation incompetent form (S656A) of GFP-DRP1. Cells were transfected with the ER marker eYFP-ER and stained with the mitochondrial dye TMRE. Results are means ± SEM of 3 separate experiments analyzing 12–34 cells per treatment. J) Electron microscopy images of wild type (WT) and *LKB1* knock out (KO) mouse β-cells in vivo. Arrows point to ER. Asterix indicates insulin granule. Size bar = 200 nm. * $P < .05$ and ** $P < .01$.

regulation of ER morphology, its role in stress-induced ER shape changes, if at all present, must be quite minor.

DRP1 regulation of ER and mitochondria morphology

Palmitate induces mitochondrial fragmentation in β-cells (22). We noticed a temporal correlation between mitochondrial fragmentation and ER expansion; this led us to postulate that common proteins coordinate morphology in these organelles. Overexpression of the mitochondrial fission protein DRP1 was reported to induce ER stress in β-cells (40), hence we studied its implication in ER morphology. The current view is that DRP1 is primarily a cytosolic protein that is recruited to mitochondrial fission sites (25). A few studies reported that DRP1 is also found in the nucleus (41), peroxisomes (42) and the ER (43). However, the role of DRP1 in the regulation of altered ER morphology in response to stress was not reported. We found that in β-cells DRP1 is localized abundantly in the ER, as well as in mitochondrial fission sites. Of note, a recent report demonstrated that fission occurs at points where ER tubules wrap around the mitochondria and mark mitochondrial division sites (11). Herein, we show that inhibition of DRP1 attenuated both mitochondria fragmentation and ER expansion induced by FFA, suggesting that these processes are coordinated, rather than being stochastic. The GTP hydrolysis-incompetent mutant (K38A) sequesters endogenous DRP1 into aggregated structures consisting of membrane tubules, thus inhibiting DRP1 localization to mitochondrial fission sites and acting as a dominant negative (44). It is thus tempting to postulate that DRP1 located at fission sites coordinates ER and mitochondria morphology and their interorganelle cross-talk. However, we cannot exclude the possibility that the effects of the K38A DRP1 mutant on ER morphology are mediated via inhibition of DRP1 in other ER subdomains. Better characterization of DRP1 assembly in the ER and recruitment to ER-mitochondria interaction sites is required to distinguish between these possibilities.

AMPK regulation of DRP1 phosphorylation and ER morphology

We identified AMPK as a major regulator of ER and mitochondria morphology in FFA-induced stress. AMPK

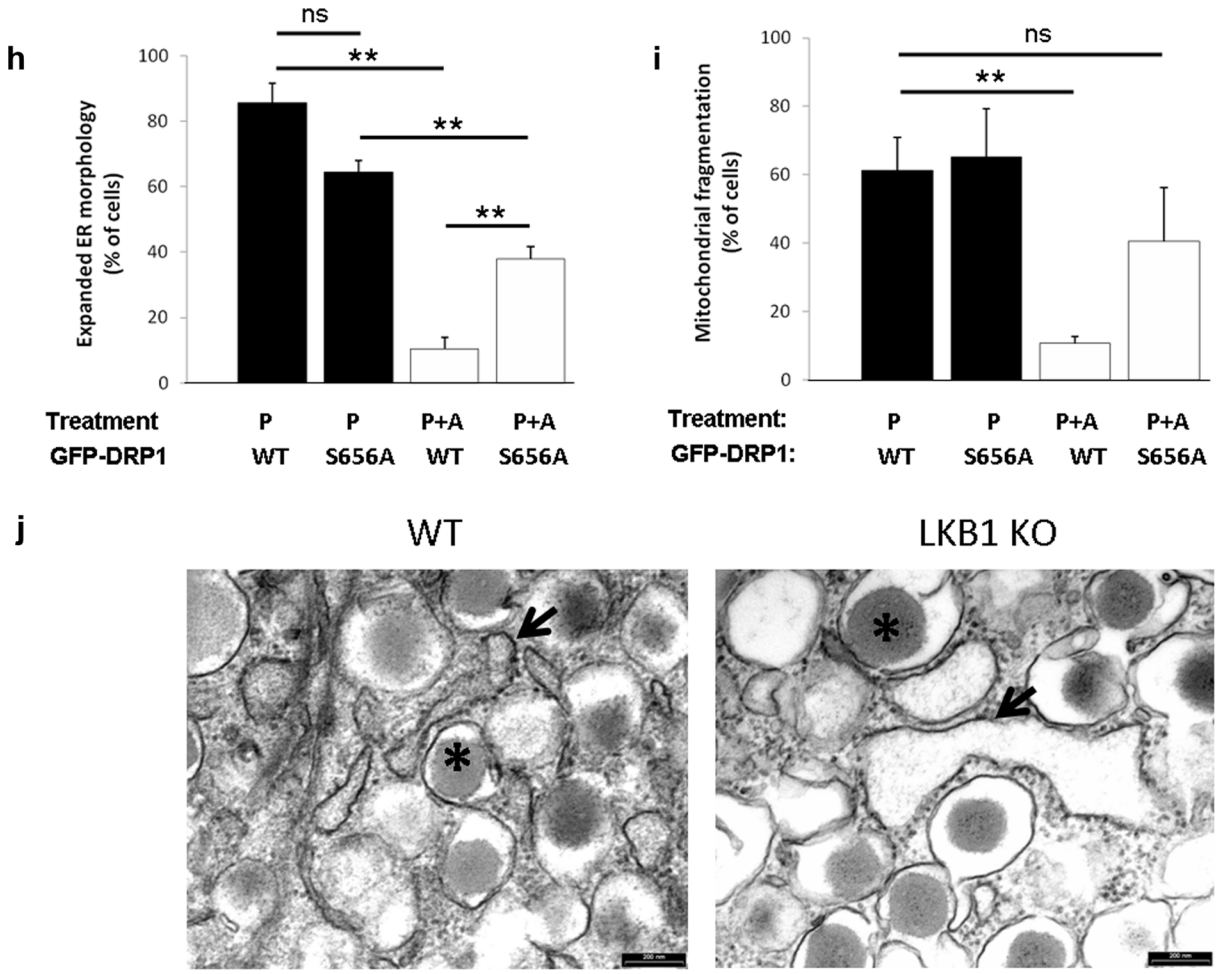

FIGURE 6B.

is a cellular energy sensor that promotes ATP production by increasing the activity or expression of proteins involved in catabolism, while switching off biosynthetic pathways to conserve ATP (28). Hitherto, the role of AMPK in the regulation of ER morphology in response to stress was unknown. We show here for the first time that AMPK regulates ER morphology: AICAR and the common T2D drug metformin, which activate AMPK (45), prevented FFA-induced ER expansion; genetic inhibition of AMPK verified that this was indeed AMPK-dependent. Moreover, the β-cell ER of mice deficient in the upstream AMPK regulator LKB1 appeared as large cisternae-like structures, suggesting that a basal AMPK activity is necessary to maintain normal ER structure in vivo. Importantly, we found that AMPK effects on ER and mitochondria morphology are mediated, at least in part, via DRP1.

Regulation of DRP1 and/or its interacting proteins by phosphorylation is important for the intra-cellular cycling of DRP1 (46). Phosphorylation of DRP1 S637 plays an important role in this context. As an example, protein kinase A (PKA) phosphorylation of DRP1 S637 was previously shown to mediate cAMP-induced mitochondrial elongation under nutrient starvation conditions (47). Conversely, calcineurin dephosphorylates DRP1 S637 and stimulates mitochondrial fragmentation (48). We show here that DRP1 is regulated by AMPK through phosphorylation of this antifission site. In line with this it was reported in lung adenocarcinoma cell lines that

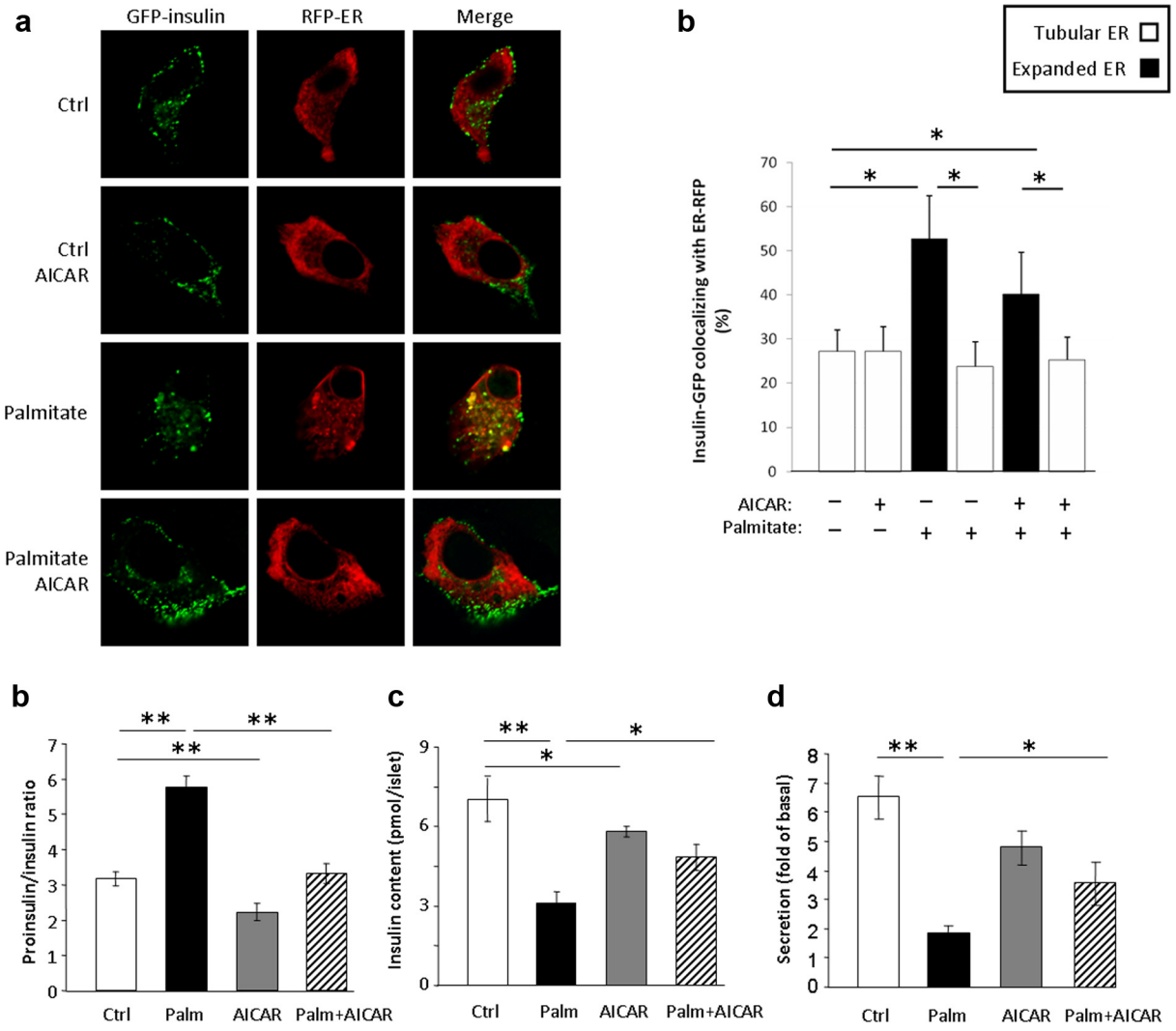

FIGURE 7. Palmitate effects on proinsulin retention in the ER and β-cell function. A) INS-1E β-cells expressing GFP-proinsulin and ER-RFP were treated as indicated at 11.1 mmol/l glucose. GFP-proinsulin/ER-RFP colocalization, indicative of proinsulin retention in the ER, was analyzed by confocal microscopy. B) Quantification of GFP-proinsulin and ER-RFP colocalization in tubular and expanded ER. Results are means ± SEM of 5 separate experiments analyzing 47 cells altogether. C-E) Effects of palmitate and AICAR on proinsulin/insulin ratio (C), insulin content (D) and secretion (E). Isolated mouse islets were treated as indicated at 11.1 mmol/l glucose for 24 h. Proinsulin and insulin were measured in islet extracts by proinsulin ELISA and insulin RIA. Insulin secretion was assessed by static incubations at 3.3 mmol/l (basal) and 16.7 mmol/l (stimulated) glucose concentrations. The ratio of stimulated/basal insulin secretion is shown. * $P < .05$; ** $P < .01$.

AMPK knockdown decreased general DRP1 phosphorylation in response to hypoxia (41). Importantly, prevention of DRP1 S637 phosphorylation partially prevented the rescuing effect of AMPK on mitochondrial fragmentation and on ER expansion. We expected that AMPK would directly phosphorylate DRP1 S637; however, at least under the in vitro test conditions used, this was not the case. Future studies will show whether AMPK regulates DRP1 phosphorylation through modifications of its interacting proteins. Of note, the prevention of AICAR effects on ER morphology by DRP1 DN or the S637 phosphorylation mutant was partial, indicating that additional mechanisms are involved in AMPK regulation of ER and mitochondria morphology. It is unlikely that AMPK effect on ER morphology is mediated via modulation of metabolism as it did not affect mitochondrial

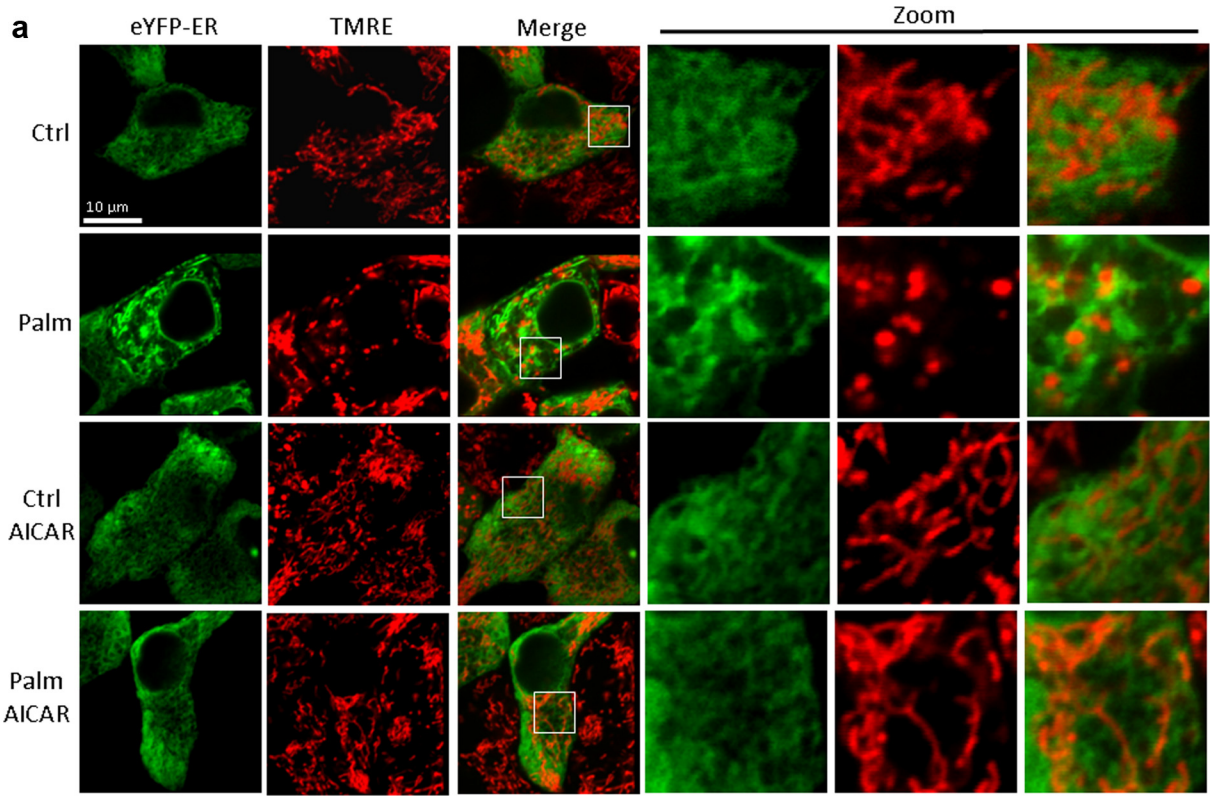

FIGURE 8A. AICAR effects on palmitate-induced mitochondrial fragmentation and apoptosis. A) INS-1E β-cells expressing eYFP-ER were treated as indicated at 11.1 mmol/l glucose (C=control, P=palmitate, A=AICAR) and then stained with the mitochondrial dye TMRE and mitochondrial fragmentation analyzed by confocal microscopy. B) Quantification of mitochondrial fragmentation. Results are means ± SEM of 5 separate experiments analyzing 155–325 cells imaged per treatment. C, D) Western blot for cleaved and total caspase-3 in INS-1E β-cells treated as indicated. A representative blot and quantification of cleaved caspase-3 at 24 h, normalized to total caspase 3 is shown. Results are means ± SEM of 3–8 separate experiments. E) Apoptosis ELISA assay quantifying nucleosome content. Results are means ± SEM of 4–5 separate experiments. * $P < .05$; ** $P < .01$.

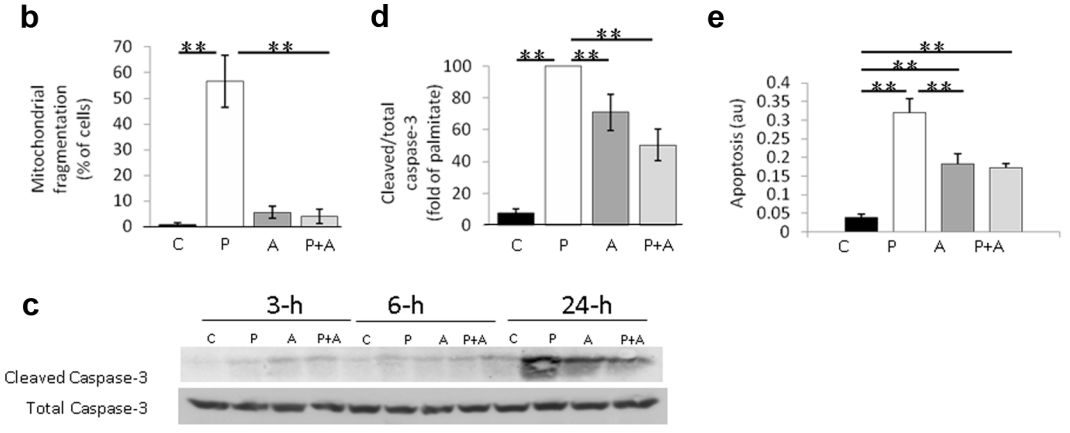

FIGURE 8B.

respiration in cells treated with palmitate (Supplemental Figure 5). Furthermore, inhibition of FFA oxidation by etomoxir did not affect the ER expansion in response to palmitate, nor did it abolish its prevention by AICAR. Similarly, inhibition of ceramide and cholesterol synthesis also failed to affect ER morphology. Of note, treatment with AICAR did not affect triglyceride levels in β-cells exposed to hyperglycemia (49), further supporting our claim that the beneficial effects of AMPK are not mediated via effects on lipid handling in the β-cell. Further studies are required to unravel DRP1-independent pathways regulating organelle morphology in stressed β-cells.

AMPK regulation of β-cell function and survival

To better understand the functional impact of the expanded cisternal ER shape on β-cell function, we developed an assay that allows assessment of proinsulin retention in the ER of single cells. We observed ER proinsulin retention in palmitate-treated cells that presented expanded ER, but not in those that retained tubular ER (Figure 6); this was associated with increased proinsulin/insulin ratio in islets. These findings are consistent with previous studies showing that palmitate inhibited ER-Golgi trafficking and proinsulin processing (50, 51). The tight correlation between ER expansion and proinsulin retention suggests a cause and effect relationship between morphology and function.

We found that AMPK stimulation by AICAR decreased basal and glucose-stimulated mitochondrial respiration and insulin secretion, and increased apoptosis. This is consistent with previous studies showing that pharmacological stimulation of AMPK increased apoptosis (52), whereas AMPK deficiency in β-cells led to augmented insulin secretion and increased β-cell mass (29, 30), The mechanisms by which AMPK stimulation generates stress and impairs β-cell function might be related to mitochondrial dysfunction and increased production of reactive oxygen species (52), although the precise mechanism is unknown. By contrast, AICAR prevented the deleterious effects of palmitate on β-cell function. In addition, AICAR decreased palmitate-induced apoptosis, in agreement with previous reports on its protective effects against lipotoxicity (53, 54). The prevention of palmitate effects on mitochondrial fragmentation and respiration, as well as on ER expansion and the associated derangements in β-cell function and survival emphasize that AMPK rescue of β-cells is specific to metabolic stress elicited by FFA. DRP1 was recently shown to mediate FFA-induced β-cell apoptosis (55). Our findings that AMPK inhibits DRP1 and prevents FFA-induced mitochondrial fragmentation and β-cell apoptosis, strongly suggest that DRP1 mediates AMPK protection of β-cells in lipotoxicity.

We conclude that the AMPK-DRP1 connection delineates a novel pathway that links metabolic stress, organelle morphology and function. AMPK preserves ER and mitochondrial structure and function in part through inhibition of DRP1, which contributes to improved β-cell function and survival. These findings have important implications for understanding the regulation of ER morphology, and for exploring novel treatments of diabetes.

Acknowledgments

This study was supported by a grant from the Israel Science Foundation to GL and by grants from the Golda Meir foundation and the EFSD to JDW. We thank the generous colleagues that provided plasmids and Dr. Orian Shirihai, Boston University, for providing *Drp1* DN adenovirus. The authors have no conflict of interest to declare.

Received April 16, 2013. Accepted August 19, 2013.

Address all correspondence and requests for reprints to: Gil Leibowitz MD, Endocrinology and Metabolism Service, Department of Medicine, Hadassah - Hebrew University Medical Center, P.O. Box 12000, Jerusalem 91120, Tel: +972–2–6777951, Fax: +972–2–6437940, E-mail: gleib@hadassah.org.il

Authors' contributions: JDW, EBW, EC and GL designed the study. JDW, TI, EBW, YA, AS and MW researched data. JDW and GL wrote the manuscript. EC reviewed and edited the manuscript and contributed to discussion. DK and YD contributed to discussion and helped with experimental design. JW is the guarantor of this work and, as such, had full access to all of the data in the study and takes responsibility for the integrity of the data and the accuracy of the data analysis.

This work was supported by.

References

1. **Wolf BA, Colca JR, Turk J, Florholmen J, McDaniel ML.** Regulation of Ca2+ homeostasis by islet endoplasmic reticulum and its role in insulin secretion. *Am J Physiol*. 1988;254:E121–136.
2. **Back SH, Kaufman RJ.** Endoplasmic reticulum stress and type 2 diabetes. *Annu Rev Biochem*. 2012;81:767–793.
3. **Cunha DA, Igoillo-Esteve M, Gurzov EN, Germano CM, Naamane N, Marhfour I, Fukaya M, Vanderwinden JM, Gysemans C, Mathieu C, Marselli L, Marchetti P, Harding HP, Ron D, Eizirik DL, Cnop M.** Death protein 5 and p53-upregulated modulator of apoptosis mediate the endoplasmic reticulum stress-mitochondrial dialog triggering lipotoxic rodent and human beta-cell apoptosis. *Diabetes*. 2012;61:2763–2775.
4. **Sachdeva MM, Claiborn KC, Khoo C, Yang J, Groff DN, Mirmira RG, Stoffers DA.** Pdx1 (MODY4) regulates pancreatic beta cell susceptibility to ER stress. *Proceedings of the National Academy of Sciences of the United States of America*. 2009;106:19090–19095.
5. **Marchetti P, Bugliani M, Lupi R, Marselli L, Masini M, Boggi U, Filipponi F, Weir GC, Eizirik DL, Cnop M.** The endoplasmic retic-

ulum in pancreatic beta cells of type 2 diabetes patients. *Diabetologia*. 2007;50:2486–2494.
6. **Peng G, Li L, Liu Y, Pu J, Zhang S, Yu J, Zhao J, Liu P.** Oleate blocks palmitate-induced abnormal lipid distribution, endoplasmic reticulum expansion and stress, and insulin resistance in skeletal muscle. *Endocrinology*. 2011;152:2206–2218.
7. **Borradaile NM, Han X, Harp JD, Gale SE, Ory DS, Schaffer JE.** Disruption of endoplasmic reticulum structure and integrity in lipotoxic cell death. *J Lipid Res*. 2006;47:2726–2737.
8. **Friedman JR, Voeltz GK.** The ER in 3D: a multifunctional dynamic membrane network. *Trends Cell Biol*. 2011;21:709–717.
9. **Hu J, Prinz WA, Rapoport TA.** Weaving the web of ER tubules. *Cell*. 2011;147:1226–1231.
10. **Shibata Y, Shemesh T, Prinz WA, Palazzo AF, Kozlov MM, Rapoport TA.** Mechanisms determining the morphology of the peripheral ER. *Cell*. 2010;143:774–788.
11. **Friedman JR, Lackner LL, West M, DiBenedetto JR, Nunnari J, Voeltz GK.** ER tubules mark sites of mitochondrial division. *Science*. 2011;334:358–362.
12. **Kageyama Y, Zhang Z, Sesaki H.** Mitochondrial division: molecular machinery and physiological functions. Current opinion in cell biology 23:427–434.
13. **Cnop M, Igoillo-Esteve M, Cunha DA, Ladriere L, Eizirik DL.** An update on lipotoxic endoplasmic reticulum stress in pancreatic beta-cells. *Biochem Soc Trans*. 2008;36:909–915.
14. **Cnop M, Ladriere L, Igoillo-Esteve M, Moura RF, Cunha DA.** Causes and cures for endoplasmic reticulum stress in lipotoxic beta-cell dysfunction. *Diabetes Obes Metab 12 Suppl*. 2010;2:76–82.
15. **Kahn SE, Hull RL, Utzschneider KM.** Mechanisms linking obesity to insulin resistance and type 2 diabetes. *Nature*. 2006;444:840–846.
16. **Cribbs JT, Strack S.** Reversible phosphorylation of Drp1 by cyclic AMP-dependent protein kinase and calcineurin regulates mitochondrial fission and cell death. *EMBO Rep*. 2007;8:939–944.
17. **Klee M, Pimentel-Muinos FX.** Bcl-X(L) specifically activates Bak to induce swelling and restructuring of the endoplasmic reticulum. *J Cell Biol*. 2005;168:723–734.
18. **Rajan S, Eames SC, Park SY, Labno C, Bell GI, Prince VE, Philipson LH.** In vitro processing and secretion of mutant insulin proteins that cause permanent neonatal diabetes. *Am J Physiol Endocrinol Metab*. 2010;298:E403–410.
19. **Korkhov VM, Zuber B.** Direct observation of molecular arrays in the organized smooth endoplasmic reticulum. *BMC Cell Biol*. 2009;10:59.
20. **Goedhart J, von Stetten D, Noirclerc-Savoye M, Lelimousin M, Joosen L, Hink MA, van Weeren L, Gadella TW, Jr., Royant A.** Structure-guided evolution of cyan fluorescent proteins towards a quantum yield of 93%. Nature communications 3:751.
21. **Twig G, Elorza A, Molina AJ, Mohamed H, Wikstrom JD, Walzer G, Stiles L, Haigh SE, Katz S, Las G, Alroy J, Wu M, Py BF, Yuan J, Deeney JT, Corkey BE, Shirihai OS.** Fission and selective fusion govern mitochondrial segregation and elimination by autophagy. *Embo J*. 2008;27:433–446.
22. **Molina AJ, Wikstrom JD, Stiles L, Las G, Mohamed H, Elorza A, Walzer G, Twig G, Katz S, Corkey BE, Shirihai OS.** Mitochondrial networking protects beta-cells from nutrient-induced apoptosis. *Diabetes*. 2009;58:2303–2315.
23. **Bachar E, Ariav Y, Ketzinel-Gilad M, Cerasi E, Kaiser N, Leibowitz G.** Glucose amplifies fatty acid-induced endoplasmic reticulum stress in pancreatic beta-cells via activation of mTORC1. *PloS one*. 2009;4:e4954.
24. **Huh WJ, Esen E, Geahlen JH, Bredemeyer AJ, Lee AH, Shi G, Konieczny SF, Glimcher LH, Mills JC.** XBP1 controls maturation of gastric zymogenic cells by induction of MIST1 and expansion of the rough endoplasmic reticulum. *Gastroenterology*. 2010;139:2038–2049.
25. **Liesa M, Palacin M, Zorzano A.** Mitochondrial dynamics in mammalian health and disease. *Physiol Rev*. 2009;89:799–845.
26. **Chang CR, Blackstone C.** Dynamic regulation of mitochondrial fission through modification of the dynamin-related protein Drp1. *Ann N Y Acad Sci*. 2010;1201:34–39.
27. **Chang CR, Blackstone C.** Drp1 phosphorylation and mitochondrial regulation. EMBO Rep. 2007;8:1088–1089; author reply 1089–1090.
28. **Hardie DG, Ross FA, Hawley SA.** AMPK: a nutrient and energy sensor that maintains energy homeostasis. *Nat Rev Mol Cell Biol*. 2012;13:251–262.
29. **Granot Z, Swisa A, Magenheim J, Stolovich-Rain M, Fujimoto W, Manduchi E, Miki T, Lennerz JK, Stoeckert CJ, Jr., Meyuhas O, Seino S, Permutt MA, Piwnica-Worms H, Bardeesy N, Dor Y.** LKB1 regulates pancreatic beta cell size, polarity, and function. *Cell Metab*. 2009;10:296–308.
30. **Fu A, Ng AC, Depatie C, Wijesekara N, He Y, Wang GS, Bardeesy N, Scott FW, Touyz RM, Wheeler MB, Screaton RA.** Loss of Lkb1 in adult beta cells increases beta cell mass and enhances glucose tolerance in mice. *Cell Metab*. 2009;10:285–295.
31. **Shen WW, Frieden M, Demaurex N.** Remodelling of the endoplasmic reticulum during store-operated calcium entry. *Biol Cell*. 2011;103:365–380.
32. **Varadarajan S, Bampton ET, Smalley JL, Tanaka K, Caves RE, Butterworth M, Wei J, Pellecchia M, Mitcheson J, Gant TW, Dinsdale D, Cohen GM.** A novel cellular stress response characterised by a rapid reorganisation of membranes of the endoplasmic reticulum. *Cell Death Differ*. 2012;19:1896–1907.
33. **Schuck S, Prinz WA, Thorn KS, Voss C, Walter P.** Membrane expansion alleviates endoplasmic reticulum stress independently of the unfolded protein response. *J Cell Biol*. 2009;187:525–536.
34. **Yoshioka M, Kayo T, Ikeda T, Koizumi A.** A novel locus, Mody4, distal to D7Mit189 on chromosome 7 determines early-onset NIDDM in nonobese C57BL/6 (Akita) mutant mice. *Diabetes*. 1997;46:887–894.
35. **Casas S, Gomis R, Gribble FM, Altirriba J, Knuutila S, Novials A.** Impairment of the ubiquitin-proteasome pathway is a downstream endoplasmic reticulum stress response induced by extracellular human islet amyloid polypeptide and contributes to pancreatic beta-cell apoptosis. *Diabetes*. 2007;56:2284–2294.
36. **Cross BC, Bond PJ, Sadowski PG, Jha BK, Zak J, Goodman JM, Silverman RH, Neubert TA, Baxendale IR, Ron D, Harding HP.** The molecular basis for selective inhibition of unconventional mRNA splicing by an IRE1-binding small molecule. *Proceedings of the National Academy of Sciences of the United States of America*. 2012;109:E869–878.
37. **Shaffer AL, Shapiro-Shelef M, Iwakoshi NN, Lee AH, Qian SB, Zhao H, Yu X, Yang L, Tan BK, Rosenwald A, Hurt EM, Petroulakis E, Sonenberg N, Yewdell JW, Calame K, Glimcher LH, Staudt LM.** XBP1, downstream of Blimp-1, expands the secretory apparatus and other organelles, and increases protein synthesis in plasma cell differentiation. *Immunity*. 2004;21:81–93.
38. **Sriburi R, Jackowski S, Mori K, Brewer JW.** XBP1: a link between the unfolded protein response, lipid biosynthesis, and biogenesis of the endoplasmic reticulum. *J Cell Biol*. 2004;167:35–41.
39. **Rubio C, Pincus D, Korennykh A, Schuck S, El-Samad H, Walter P.** Homeostatic adaptation to endoplasmic reticulum stress depends on Ire1 kinase activity. *J Cell Biol*. 2011;193:171–184.
40. **Peng L, Men X, Zhang W, Wang H, Xu S, Xu M, Xu Y, Yang W, Lou J.** Dynamin-related protein 1 is implicated in endoplasmic reticulum stress-induced pancreatic beta-cell apoptosis. *Int J Mol Med*. 2011;28:161–169.
41. **Chiang YY, Chen SL, Hsiao YT, Huang CH, Lin TY, Chiang IP, Hsu WH, Chow KC.** Nuclear expression of dynamin-related protein 1 in lung adenocarcinomas. *Mod Pathol*. 2009;22:1139–1150.
42. **Koch A, Thiemann M, Grabenbauer M, Yoon Y, McNiven MA,**

Schrader M. Dynamin-like protein 1 is involved in peroxisomal fission. *J Biol Chem*. 2003;278:8597–8605.
43. **Yoon Y, Pitts KR, Dahan S, McNiven MA.** A novel dynamin-like protein associates with cytoplasmic vesicles and tubules of the endoplasmic reticulum in mammalian cells. *J Cell Biol*. 1998;140:779–793.
44. **Yoon Y, Pitts KR, McNiven MA.** Mammalian dynamin-like protein DLP1 tubulates membranes. *Molecular biology of the cell*. 2001;12:2894–2905.
45. **Owen MR, Doran E, Halestrap AP.** Evidence that metformin exerts its anti-diabetic effects through inhibition of complex 1 of the mitochondrial respiratory chain. *Biochem J*. 2000;348 Pt 3:607–614.
46. **Otera H, Ishihara N, Mihara K.** New insights into the function and regulation of mitochondrial fission. *Biochimica et biophysica acta*. 2013;1833:1256–1268.
47. **Rambold AS, Kostelecky B, Elia N, Lippincott-Schwartz J.** Tubular network formation protects mitochondria from autophagosomal degradation during nutrient starvation. *Proceedings of the National Academy of Sciences of the United States of America*. 2011;108:10190–10195.
48. **Cereghetti GM, Stangherlin A, Martins de Brito O, Chang CR, Blackstone C, Bernardi P, Scorrano L.** Dephosphorylation by calcineurin regulates translocation of Drp1 to mitochondria. *Proceedings of the National Academy of Sciences of the United States of America*. 2008;105:15803–15808.
49. **Nyblom HK, Sargsyan E, Bergsten P.** AMP-activated protein kinase agonist dose dependently improves function and reduces apoptosis in glucotoxic beta-cells without changing triglyceride levels. *J Mol Endocrinol*. 2008;41:187–194.
50. **Boslem E, MacIntosh G, Preston AM, Bartley C, Busch AK, Fuller M, Laybutt DR, Meikle PJ, Biden TJ.** A lipidomic screen of palmitate-treated MIN6 beta-cells links sphingolipid metabolites with endoplasmic reticulum (ER) stress and impaired protein trafficking. *Biochem J*. 2011;435:267–276.
51. **Preston AM, Gurisik E, Bartley C, Laybutt DR, Biden TJ.** Reduced endoplasmic reticulum (ER)-to-Golgi protein trafficking contributes to ER stress in lipotoxic mouse beta cells by promoting protein overload. *Diabetologia*. 2009;52:2369–2373.
52. **Cai Y, Martens GA, Hinke SA, Heimberg H, Pipeleers D, Van de Casteele M.** Increased oxygen radical formation and mitochondrial dysfunction mediate beta cell apoptosis under conditions of AMP-activated protein kinase stimulation. *Free Radic Biol Med*. 2007;42:64–78.
53. **Lu J, Wang Q, Huang L, Dong H, Lin L, Lin N, Zheng F, Tan J.** Palmitate causes endoplasmic reticulum stress and apoptosis in human mesenchymal stem cells: prevention by AMPK activator. *Endocrinology*. 2012;153:5275–5284.
54. **Mayer CM, Belsham DD.** Palmitate attenuates insulin signaling and induces endoplasmic reticulum stress and apoptosis in hypothalamic neurons: rescue of resistance and apoptosis through adenosine 5′ monophosphate-activated protein kinase activation. *Endocrinology*. 2010;151:576–585.
55. **Peng L, Men X, Zhang W, Wang H, Xu S, Fang Q, Liu H, Yang W, Lou J.** Involvement of dynamin-related protein 1 in free fatty acid-induced INS-1-derived cell apoptosis. *PLoS one*. 2012;7:e49258.